O. Hahtela, K. Nera and I. Tittonen, Position measurement of a cavity mirror using polarization spectroscopy, Journal of Optics A: Pure and Applied Optics 6, S115-S120 (2004).

INSTITUTE OF PHYSICS PUBLISHING JOURNAL OF OPTICS A: PURE AND APPLIED OPTICS

J. Opt. A: Pure Appl. Opt. **6** (2004) S115–S120 PII: S1464-4258(04)69073-8

Position measurement of a cavity mirror using polarization spectroscopy

O Hahtela, K Nera and I Tittonen

Metrology Research Institute, Helsinki University of Technology, PO Box 3000, FIN-02015 HUT, Finland

E-mail: ossi.hahtela@hut.fi

Received 15 September 2003, accepted for publication 12 January 2004
Published 24 February 2004
Online at stacks.iop.org/JOptA/6/S115 (DOI: 10.1088/1464-4258/6/3/019)

Abstract

A high-reflectivity coated mechanical silicon oscillator with high quality value of the mechanical resonance was employed as a planar rear mirror in a Fabry–Perot interferometer. Active stabilization of the interferometer improves the stability of the resonance and makes it possible to perform sensitive interferometric measurements. The frequency locking of lasers to optical cavities requires typically the generation of an error signal with a typical steep slope at resonance. The Hänsch–Couillaud locking method utilizes polarization spectroscopy by monitoring changes in the polarization of the light field reflected from the cavity. A polarization analyser detects dispersion shaped resonances which give the error signal for the electronic servo loop. The error signal contains information about the changes in the cavity length and thus the motion of the mechanical oscillator can be observed. The error signal was detected with the use of a spectrum analyser. The noise floor of the interferometer response indicates that the sensitivity of the optomechanical sensor or the minimum observable displacement in the mechanical oscillator position is $\Delta x_{\min} = 1.7 \times 10^{-14}$ m. This gives high enough sensitivity to observe the Brownian motion of the oscillator at room temperature.

Keywords: high-Q mechanical oscillator, optical interferometry, optomechanical sensor

(Some figures in this article are in colour only in the electronic version)

1. Introduction

High-Q oscillators are mechanical structures with spectrally very narrow mechanical resonance. The response of a resonant system is proportional to the inverse of the resonance spectral width, which motivates the pursuit of very narrow resonances. Narrow spectral width of a mechanical resonance is usually characterized by a high Q-value. Such resonances are very sensitive to changes in the physical parameters of the environment [1, 2]. Thus, mechanical resonators that have stable resonance with high Q-value can be utilized e.g. in realizing reference oscillators, filters and sensors for acceleration, pressure, absorption, temperature, force etc.

More applications can be found for example in detection of gravitational waves [3, 4], radiation pressure [5], atomic force microscopes (AFM) [6] and in sophisticated high-precision experiments for observing quantum effects. Such effects are e.g. quantum back action of the probe laser beam and the fundamental Heisenberg uncertainty based limit (standard quantum limit, SQL) of the sensitivity in measuring the position of a macroscopic body [7–9].

A very sensitive and low-noise detection system is needed to observe small displacements in the position of a high-Q mechanical oscillator. A convenient detection method is to make use of optical interferometry, in which a mechanical oscillator is integrated into the optical resonator as one of the two mirrors. Employing simultaneously a narrow mechanical resonance of a high-Q oscillator and a high-finesse optical cavity of a Fabry–Perot interferometer, extremely good resonant force detection sensitivity can be achieved. Besides

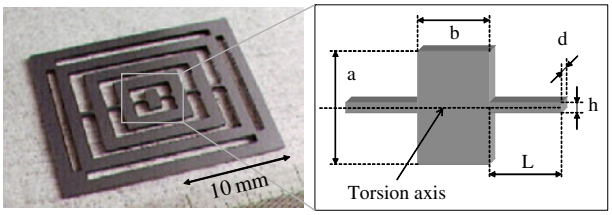

Figure 1. Torsional mechanical silicon oscillator. Oscillator dimensions are $a = 2.3$ mm, $b = 1.4$ mm, $h = 200$ μm, $d = 380$ μm and $L = 1.2$ mm.

detecting the oscillator motion, optomechanical coupling offers possibilities e.g. to freeze the mirror motion by an additional radiation pressure applied on the mirror (cold damping) or to squeeze the thermal noise by parametric amplification [10–12]. There have also been experimental proposals for demonstrating quantum mechanical effects on a macroscopic body, e.g. producing and observing macroscopic superpositions of a mirror in an optomechanical system [13].

An alternative method to measure or excite mechanical motion of high-Q oscillators is to use capacitive coupling [1, 14]. Most recent development of capacitive high-frequency mechanical oscillators has revealed extremely low phase noise levels and relatively high Q-values despite very small overall size. Optical methods, however, make it possible to entangle the light field amplitude of the optical resonator to the position coordinate of the oscillator.

2. Mechanical oscillator as a moving mirror

The oscillator used in this work can be considered to behave like a one-dimensional mechanical harmonic oscillator in a pure torsional mode. The oscillator structure is shown in figure 1. Torsional oscillators with a high Q-value have proven to be very feasible and powerful instruments in a wide variety of measurement applications [2, 14]. A torsional mode oscillation typically introduces only very little internal damping and leads thus to a high Q-value [1]. Furthermore, no considerable local volume changes are present in a weak torsional motion (thermoelastic losses are negligible) and the coupling to the clamping losses is also rather low.

In our configuration, the actual oscillator is a balanced torsionally vibrating rectangular silicon vane ($1.4 \times 2.3 \times 0.38$ mm^3) which is mounted with 200 μm narrow bridges to several surrounding frames. The purpose of combining several frames around the oscillator is to decouple the inner oscillator from the clamping and to minimize energy losses from the mechanical oscillation even more effectively than with the design used in [1]. Additional frames are torsionally vibrating oscillators as well, but due to the much larger mass their resonance frequencies differ considerably from that of the inner vane resonance.

Oscillators were fabricated from single-crystal silicon due to excellent elastic properties and low intrinsic mechanical losses [14]. Components were produced from double-sided polished (DSP), (100) oriented silicon wafers (p-type, 5–10 Ω cm) by etching from both sides simultaneously in a 25% TMAH solution at 85 °C. A thermal silicon oxide layer has been utilized as an etching mask. Double-sided anisotropic wet etching has been used in order to produce symmetrical components with well defined features and high surface quality which are of the essence in minimizing energy dissipation. Wafer thickness and the corner compensation structures required in wet etching of silicon and anisotropic wet etching itself set a limitation to the minimum feature sizes of the oscillators. Moreover, decreasing the overall component size increases the surface to volume ratio and leads to increased intrinsic losses [15].

The oscillator was characterized before depositing the dielectric high-reflective coating on the oscillator surface. In a low-pressure environment ($p < 10^{-3}$ mbar) the resonance frequency was measured to be $f_0 = 67\,668$ Hz and Q-value 750 000. At cryogenic temperature ($T = 4.2$ K) the highest measured Q-value for our torsionally vibrating structures exceeded 2.1×10^6.

The resonance frequency ω_0 of a mechanical oscillator can be calculated with its spring constant k and mass m, $\omega_0 = (k/m)^{1/2}$. Moment of inertia Θ of the mechanical torsional oscillator is needed in order to determine the oscillator effective mass $m_{\mathrm{eff}} = \Theta/l^2$ at the distance l off the torsion axis. The moment of inertia can be calculated if the dimensions of the oscillator and the density ρ of the material are known [1]

$$\Theta = \frac{2}{3}\rho_{\mathrm{Si}}\left(\frac{a}{2}\right)^3 bd, \tag{1}$$

where dimensions a, b and d are as described in figure 1. Moments of inertia of the two bridges are small (by a factor of 100) compared to that of the oscillator and can be ignored here.

The linear equation of motion for a torsional mechanical oscillation is

$$\Theta\ddot{\theta} + c\dot{\theta} + \kappa\theta = \tau(t), \tag{2}$$

where θ is the rotation angle, c is the damping constant, κ describes the torsional restoring constant of the two silicon bridges and $\tau(t)$ is external torque.

2.1. Mechanical susceptibility

The mechanical susceptibility $\chi(\omega)$ gives the frequency response of the mechanical system when an external oscillatory force $F = F_0\cos(\omega t)$ is acting on it. The oscillator will be forced to oscillate with the angular frequency ω of the applied force. In the case of a mechanical harmonic oscillator, the mechanical susceptibility has a Lorentzian behaviour and it can be written as

$$\chi(\omega) = \frac{1}{m(\omega_0^2 - \omega^2 - \mathrm{i}\omega\omega_0/Q)}, \tag{3}$$

where ω is the angular frequency of the external excitation force. From equation (3) one can derive the magnitude of the oscillation amplitude $\Delta x(\omega)$, assuming that the excitation force is monochromatic

$$\Delta x(\omega) = \frac{F_0}{m\sqrt{(\omega_0^2 - \omega^2)^2 + (\omega\omega_0/Q)^2}}. \tag{4}$$

2.2. Spectral power density and thermal excitation

Thermomechanical noise can be the limiting noise component in many conventional micromachined systems that require high precision and sensitivity [16]. The coupling of a mechanical oscillator to the heat bath leads to energy loss and noise according to the fluctuation–dissipation theorem. The energy dissipation transforms the mechanical energy of an oscillating system into thermal energy. On the other hand, the thermal energy of the environment (thermal bath) produces a random excitation to the oscillator, which causes fluctuations in the oscillator motion known as Brownian motion. Thermal noise, which is basically white noise with a flat spectrum, can excite a detectable displacement in the mechanical high-Q oscillator position at the oscillator resonance frequency.

The Nyquist relation gives the spectral density of the fluctuating force $S_{\mathrm{F}}(\omega)$ driving a mechanical resonance [17]

$$S_{\mathrm{F}}(\omega) = 4k_{\mathrm{B}}Tc = \frac{4k_{\mathrm{B}}Tm\omega_0}{Q}, \tag{5}$$

where k_{B} is the Boltzmann constant, T is temperature and c is the damping constant of the oscillation. For a harmonic mechanical oscillator, the damping constant is equal to $c = m\omega_0/Q$. If equation (5) is multiplied by the square of the modulus of the dynamical susceptibility $\chi(\omega)$ given in equation (3), the spectral density of the deviation in the oscillator position $S_{\mathrm{TH}}(\omega)$ due to the thermal excitation is obtained by

$$\begin{aligned} S_{\mathrm{TH}}(\omega) &= |\chi(\omega)|^2 S_{\mathrm{F}}(\omega) \\ &= \frac{1}{m^2(\omega^2-\omega_0^2)^2 + m^2\omega^2\omega_0^2/Q^2}\frac{4k_{\mathrm{B}}Tm\omega_0}{Q}. \end{aligned} \tag{6}$$

At the oscillator resonance frequency $\omega = \omega_0$ and equation (6) becomes

$$S_{\mathrm{TH}}(\omega_0) = \frac{4k_{\mathrm{B}}TQ}{m\omega_0^3}. \tag{7}$$

The mass of the oscillator can be replaced by the effective mass $m = m_{\mathrm{eff}} = \Theta/l^2$. Now equation (7) can be used to calculate the displacement in the oscillator position

$$\sqrt{S_{\mathrm{TH}}} = \sqrt{\frac{4k_{\mathrm{B}}TQl^2}{\Theta\omega_0^3}}, \tag{8}$$

where l indicates the distance of the inspected point, i.e. the point where the laser beam is focused from the torsion axis. The moment of inertia Θ of the oscillator can be calculated from equation (1). With the parameters of the oscillator, $Q = 16\,500$, $\omega_0 = 2\pi \times 67\,668$ Hz, $l = 1$ mm, $T = 300$ K and $\Theta = 1.24 \times 10^{-12}$ kg m^2, equation (8) gives

$$\sqrt{S_{\mathrm{TH}}} = 5.4 \times 10^{-14}\ \mathrm{m\ Hz^{-1/2}}. \tag{9}$$

3. Interferometer set-up and frequency stabilization

An HR-coated mechanical silicon oscillator is employed as a planar rear mirror in a Fabry–Perot interferometer (figure 2). The essence of the method lies in monitoring the changes in the interferometer response driven by the physical oscillations of the mechanical oscillator. The error signal of the active stabilization serves as a control feedback signal and it contains

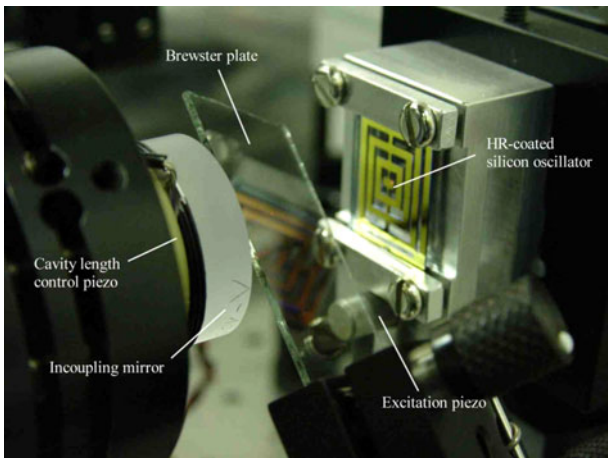

Figure 2. an HR-coated high-Q oscillator is employed as a planar rear mirror in a Fabry–Perot interferometer. The length of the cavity can be controlled by a ring piezo-actuator mounted on the incoupling mirror. The high-Q oscillator can be mechanically excited by another piezo-actuator attached to the aluminium oscillator mount.

information about dynamic length variations of the optical cavity. It is, however, important to notice that a Fabry–Perot interferometer itself is sensitive to any length variations of the optical cavity whereas the high-Q oscillator is sensitive only to forces at its resonance frequency.

In our configuration, a HeNe laser provides linearly polarized 5 mW output power (TEM_{00}-mode) at the wavelength of $\lambda = 632.8$ nm. The frequency stability of the HeNe laser was measured by comparing it to an additional high-precision iodine stabilized HeNe laser. According to our measurements the electronic feedback circuit was observed to be fast enough to compensate the cavity length change due to the frequency drift of 100 kHz s^{-1}. Laser beam intensity noise (rms) is less than 0.2% (<10 MHz) and polarization ratio is better than 500:1. The length of the optical cavity is 25 mm; the amplitude reflection coefficients of the incoupling mirror and the HR coated oscillator are $r_1 = 0.99$ and $r_2 = 0.98$, respectively, giving a moderate optical finesse of $\mathcal{F} = 100$, a free spectral range of $\Delta\nu_{\mathrm{FSR}} = 6$ GHz and a mode width of $\nu_{\mathrm{h}} = 60$ MHz. The radius of curvature of the concave incoupling mirror is 100 mm and the beam waist at the plane oscillator mirror is $w_0 = 93\ \mu$m.

We use the Hänsch–Couillaud locking method [18] to stabilize the interferometer to the laser frequency (figure 3). This method utilizes polarization spectroscopy and the changes in the polarization of the reflected light are monitored. A deviation in the phase of the incident laser beam relative to the light field stored inside the optical cavity alters the polarization of the reflected light. The reflected light faces a frequency-dependent elliptical polarization. A polarization analyser detects dispersion shaped resonances which give the error signal for the electronic servo loop. Several other methods for frequency locking are available, e.g. frequency-modulation (FM) spectroscopy or the Pound–Drewer–Hall technique [19–21], but Hänsch–Couillaud locking provides a convenient method with no need for phase or frequency modulation and thus additional electronics and noise sources can be avoided. A disadvantage of the Hänsch–Couillaud method is that it requires an intracavity polarizer which in our configuration

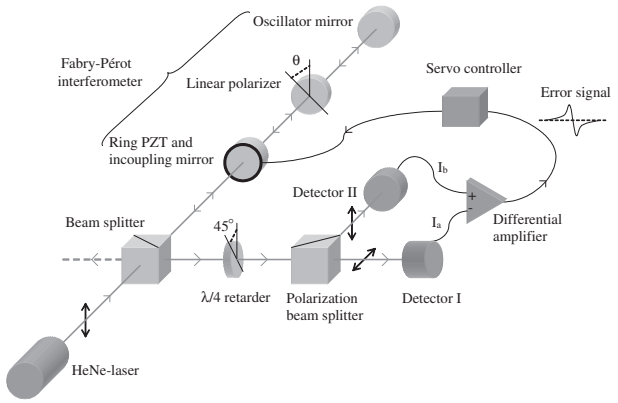

Figure 3. The Hänsch–Couillaud locking method is based on polarization spectroscopy. Dispersion shaped resonances provide the error signal for the electronic servo loop.

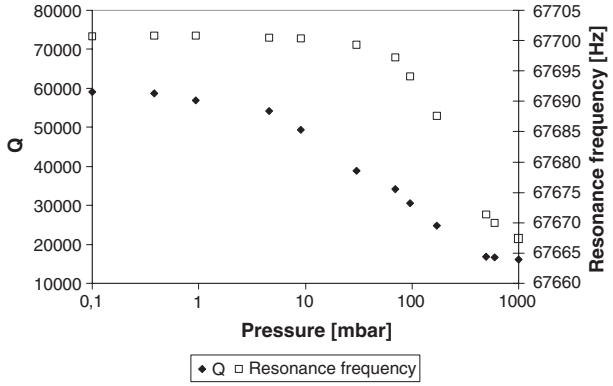

Figure 4. The optical cavity was placed in a vacuum chamber and the oscillator resonance frequency and Q-value were measured as a function of pressure.

is a Brewster plate. Although a Brewster cut crystal has the advantage of allowing low reflection losses it inevitably limits the obtainable finesse of the cavity to a modest level.

The Fabry–Perot interferometer is coherently driven with a single-mode HeNe laser. Linearly polarized light is reflected from the optical cavity. The transmission axis of the intracavity linear polarizer forms an angle θ with the polarization axis of the linearly polarized incident laser beam. The incoming light has two orthogonal linearly polarized components. The electric field vector of the other component is parallel and the electric field vector of the other component is perpendicular to the transmission axis of the linear polarizer. The parallel component faces a cavity with minimum losses and experiences a frequency-dependent phase shift δ in the reflection. The perpendicular field component just reflects from the incoupling mirror and it serves as a reference signal.

Exactly at the resonance ($\delta = 2m\pi$), the reflected intensity has its minimum (inverse of the Airy function) and the reflected beam is linearly polarized. If the resonance condition is not fulfilled, the reflected parallel component has a phase shift relative to the perpendicular component and thus the reflected beam faces an elliptical polarization. The ellipticity of the polarization can be detected with a polarization analyser which consists of a quarter wave retarder and a linear polarization beamsplitter.

The outputs of the polarization analyser, light intensities I_a and I_b, are detected with silicon photodiodes and connected to the differential amplifier. The output signal of the differential amplifier provides an error signal with a steep slope at resonance and far reaching wings. This error signal is used for the electronic cavity length control and for the interferometer response analysis. The mathematical form of the error signal is given in [18]

$$I_a - I_b = I^{(i)} 2 \cos\theta \sin\theta \frac{T_1 R \sin\delta}{(1-R)^2 + 4R\sin^2(\frac{1}{2}\delta)}, \qquad (10)$$

where $I^{(i)}$ is the intensity of the incident laser beam, T_1 is the power transmissivity of the incoupling mirror and R is the amplitude ratio between successive roundtrips containing the reflection and any other losses inside the cavity.

An ordinary PID controller was utilized as an electronic servo loop. It should be noted here that the bandwidth of the electronic feedback must not include the resonance frequency of the mechanical silicon oscillator. Otherwise the cavity locking system would try to compensate the cavity length changes caused by the oscillator motion. Moreover, due to the high mechanical quality of the oscillator, the control process exactly at the resonance frequency could introduce some unwanted excitation for the silicon oscillator.

4. Measurements and results

The behaviour of the HR-coated mechanical silicon oscillator was studied as a function of pressure (figure 4). The measurement shows that Q-value increases significantly as the pressure decreases and saturates to its maximum value. Gas damping of the surrounding media is the main reason for the energy losses of the oscillation and the highest Q-values can be achieved only in high vacuum. The mechanical Q-value was determined from the decay time τ of the resonance. The oscillator was mechanically excited to vibrate at its resonance frequency by a function generator driven piezo-actuator which was attached to the oscillator mount (figure 2). The oscillation amplitude was allowed to saturate to the level which is proportional to the strength of the harmonic external excitation force. After cutting off the excitation, the oscillation started decaying and the envelope curve of the exponentially damped oscillation was stored with a SRS 830 dual-phase lock-in amplifier from the error signal. The Q-value can be calculated from the decay time and the resonance frequency f_0 ($Q = \pi\tau f_0$).

The response of the optomechanical sensor was studied next. The excitation piezo was driven with a sinusoidal voltage at the mechanical resonance frequency of $f_0 = 67\,668.8$ Hz and $V = 100\ \mathrm{mV_{pp}}$ through a variable attenuator. Attenuation levels used here were 50, 80, 100 and 110 dB, which gave the excitation amplitudes of 316, 10, 1 and 0.316 $\mu\mathrm{V_{pp}}$, respectively. The error signal was Fourier transformed and recorded by a SRS 760 FFT spectrum analyser. The frequency responses with different excitation amplitudes are shown in figure 5. The overall measurement frequency span was about 50 Hz, giving a resolution of 120 mHz for each calculated FFT. Moreover, the spectrum was averaged 100 times. The interferometer response was shown to increase linearly with

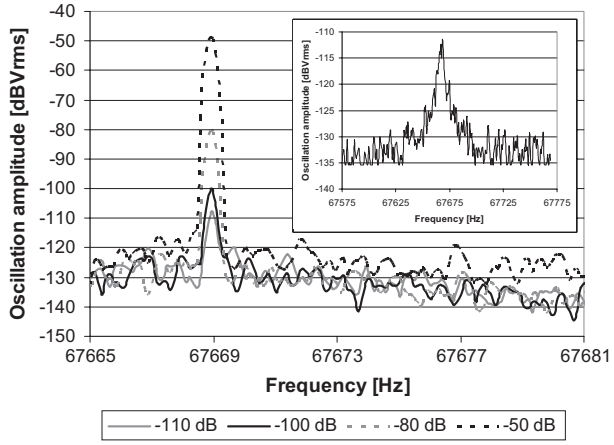

Figure 5. Frequency response of the interferometer with the oscillator resonance being mechanically excited at various excitation levels showing linear behaviour. The inset shows clearly detectable thermally excited oscillator motion at 300 K.

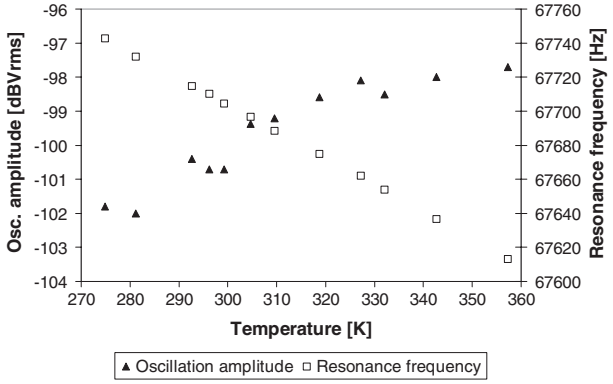

Figure 6. The operating temperature of the oscillator was altered with Peltier elements attached to the oscillator mount. Measurements were carried out at the pressure of 1 mbar.

the excitation amplitude if the oscillator was excited to vibrate at a moderate level.

Because of the linear behaviour of the interferometer response, the amplitude of the excitation signal and, therefore, the displacement in the oscillator position can be calculated if the oscillation amplitude is known. According to the measurement shown in the inset of figure 5 the oscillation amplitude of -112 dB V_{rms} due to the thermal excitation corresponds to an excitation amplitude of 250 nV_{pp} and a displacement of the oscillator of $\Delta x_{thermal} = 1.9 \times 10^{-13}$ m. This result is in fairly close agreement with the theoretical consideration discussed earlier in section 2.2, since multiplying equation (9) by the square root of the measurement bandwidth one can evaluate the theoretical oscillator displacement to be $\Delta x_{theoretical} = 1.1 \times 10^{-13}$ m. Here the measurement bandwidth is equal to the spectral width of the thermally excited oscillation $\Delta f = 4.1$ Hz which is determined from the measurement data and from the definition of the Q-value ($Q = f_0/\Delta f$). The noise floor of the interferometer response (-133 dB V_{rms}) close to the resonance frequency indicates that the minimum detectable displacement in the high-Q oscillator position in our case is $\Delta x_{min} = 1.7 \times 10^{-14}$ m or equivalently $S_{min}^{1/2} = \Delta x_{min}/\Delta f^{1/2} = 8.4 \times 10^{-15}$ m $Hz^{-1/2}$.

In addition, two Peltier thermoelectric modules were attached to the oscillator mount and the interferometer response to thermal excitation was studied at different temperatures and under the pressure of 1 mbar (figure 6). The resonance frequency of the oscillator was decreased by 0.2 % as the operating temperature was increased by 80 K from 275 K (25 ppm K^{-1}). This was expected because the elastic constant of silicon decreases at higher temperatures. Similar results can be found e.g. in [1]. The growth in oscillation amplitude due to the increased thermal excitation was clearly observed as shown in figure 6.

5. Discussion

The research group from *Laboratoire Kastler Brossel* in France has also reported high-sensitivity optical measurements for the mechanical motion of an oscillator mirror [10, 11, 22–24]. However, their approach to the subject is somewhat different from ours. The moving mirror in their experiments is an HR coated plano-convex mechanical silica resonator vibrating in a Gaussian internal acoustic mode. Phase fluctuations in the light field reflected by the cavity are measured by the homodyne technique. In their room-temperature experiment, the mechanical resonance frequency of the mirror is close to 2 MHz, the Q-value is 44 000 and the finesse is 37 000. With these parameters the minimum observable oscillator displacement was reported to be 2×10^{-19} m $Hz^{-1/2}$ [22]. This value shows remarkably better sensitivity than ours ($S_{min}^{1/2} = 8.4 \times 10^{-15}$ m $Hz^{-1/2}$). However, additional measurements are planned to investigate the possibilities of increasing the sensitivity of our optomechanical sensor by several orders of magnitude.

Higher sensitivities can be achieved by increasing the mechanical Q-value of the oscillator. We discovered that the influence of the required HR coating on the Q-value was distinctly larger than expected. Reducing the coated area should make it possible to maintain the initially high Q-value. If the system is cooled down to cryogenic temperatures, many intrinsic energy losses of the oscillator, such as thermoelastic dissipation, have only minor effects, and higher Q-values can be achieved. At 4.2 K our highest measured Q-value exceeded $Q = 2.1 \times 10^6$. Moreover, using microresonators fabricated on the silicon-on-insulator (SOI) wafer, the mass of the oscillator can be reduced substantially, which leads to the ability to detect smaller forces acting on the oscillator.

6. Conclusions

A very sensitive optomechanical sensor based on optical interferometry was designed, constructed and tested. It was demonstrated experimentally that a high-Q mechanical silicon oscillator vibrating in a torsional mode can be used in high-precision measurements. The Hänsch–Couillaud locking method was realized and shown to stabilize the Fabry–Perot interferometer with a good enough accuracy, so that this method can obviously be used in estimating the potentiality of the oscillators used in the detection of ultraweak mechanical forces. The measured noise floor of the interferometer response indicates that the minimum detectable oscillator

displacement in this case is $S_{\min}^{1/2} = 8.4 \times 10^{-15}$ m Hz$^{-1/2}$, which is low enough that the observation of the high-Q mechanical mode excited only with thermal energy is obvious.

References

[1] Buser R A and Rooij N F 1990 Very high Q-factor resonators in monocrystalline silicon *Sensors Actuators* A **21–23** 323–7

[2] Kleinman R N, Kaminsky G K, Reppy J D, Pindak R and Bishop D J 1985 Single-crystal silicon high-Q torsional oscillators *Rev. Sci. Instrum.* **56** 2088

[3] Caves C M 1980 Quantum-mechanical radiation-pressure fluctuations in an interferometer *Phys. Rev. Lett.* **45** 75

[4] Pang Y and Richard J-P 1995 Room-temperature tests of an optical transducer for resonant gravitational wave detectors *Appl. Opt.* **34** 4982

[5] Dorsel A, McCullen J D, Meystre P, Vignes E and Walther H 1983 Optical bistability and mirror confinement induced by radiation pressure *Phys. Rev. Lett.* **51** 1550

[6] Albrecht T R, Grütter P, Horne D and Rugar D 1991 Frequency modulation detection using high-Q cantilevers for enhanced force microscope sensitivity *J. Appl. Phys.* **69** 668

[7] Milburn G J, Jacobs K and Walls D F 1994 Quantum-limited measurements with the atomic force microscope *Phys. Rev.* A **50** 5256

[8] Jacobs K, Tittonen I, Wiseman H M and Schiller S 1999 Quantum noise in the position measurement of a cavity mirror undergoing Brownian motion *Phys. Rev.* A **60** 538

[9] Tittonen I, Breitenbach G, Kalkbrenner T, Müller T, Conradt R, Schiller S, Steinsland E, Blanc N and de Rooij N F 1999 Interferometric measurements of the position of a macroscopic body: towards observation of quantum limits *Phys. Rev.* A **59** 1038

[10] Cohadon P F, Heidmann A and Pinard M 1999 Cooling of a mirror by radiation pressure *Phys. Rev. Lett.* **83** 3174

[11] Briant T, Cohadon P F, Pinard M and Heidmann A 2003 Optical phase-space reconstruction of mirror motion at the attometer level *Eur. Phys. J.* D **22** 131–40

[12] Vitali D, Mancini S, Ribichini L and Tombesi P 2003 Macroscopic mechanical oscillators at the quantum limit through optomechanical cooling *J. Opt. Soc. Am.* B **20** 1054

[13] Marshall W, Simon C, Penrose R and Bouwmeester D 2003 Towards quantum superpositions of a mirror *Phys. Rev. Lett.* **91** 130401

[14] Petersen K E 1982 Silicon as a mechanical material *Proc. IEEE* **70** 420

[15] Mihailovich R E and MacDonald N C 1995 Dissipation measurements of vacuum-operated single-crystal silicon microresonators *Sensors Actuators* A **50** 199–207

[16] Gabrielson T B 1993 Mechanical-thermal noise in micromachined acoustic and vibration sensors *IEEE Trans. Electron Devices* **40** 903

[17] Kittel C 1958 *Elementary Statistical Physics* (New York: Wiley) p 141

[18] Hänsch T W and Couillaud B 1980 Laser frequency stabilization by polarization spectroscopy of a reflecting reference cavity *Opt. Commun.* **35** 441

[19] Bjorklund G C 1980 Frequency-modulation spectroscopy: a new method for measuring weak absorptions and dispersions *Opt. Lett.* **5** 15

[20] Bjorklund G C, Levenson M D, Lenth W and Ortiz C 1983 Frequency modulation (FM) spectroscopy *Appl. Phys.* B **32** 145

[21] Drewer R W P, Hall J L, Kowalski F V, Hough J, Ford G M, Munley A J and Ward H 1983 Laser phase and frequency stabilization using an optical resonator *Appl. Phys.* B **31** 97

[22] Hadjar Y, Cohadon P F, Aminoff C G, Pinard M and Heidmann A 1999 High-sensitivity optical measurement of mechanical Brownian motion *Europhys. Lett.* **47** 545–51

[23] Heidmann A, Hadjar Y and Pinard M 1997 Quantum nondemolition measurement by optomechanical coupling *Appl. Phys.* B **64** 173–80

[24] Pinard M, Hadjar Y and Heidmann A 1999 Effective mass in quantum effects of radiation pressure *Eur. Phys. J.* D **7** 107–16